

The Quincunx Filter-Based Sharp Frequency Localized Contourlet Transform for Image Denoising

Asst. Lec. Nidaa H. Abbas

Electrical Engineering Department, college of Engineering
Al-Mustansiria University

Abstract

The contourlet transform, one of the recent geometrical transform offers the two important features of anisotropy scaling law and directionality, but non-ideal filters are used which results in two important problems, first is the pseudo-Gibbs phenomena around singularities produced by the Laplacian pyramid stage. Sharp frequency localized contourlet transform (SFLCT) is a new construction contourlet which succeeded in solving this problem by replacing the Laplacian pyramid with a new multiscale decomposition defined in the frequency domain. But the shift variant, the second problem was not solved by this work due to the downsampling of Laplacian pyramid and DFB stages. In this work, a high-performance quincunx filter banks are used in the DFB stage of SFLCT and noble identity is employed to solve the problem introduced by the downsampler and upsampler. The simulations illustrate significant improvements under the proposed transform when compared with other transform variations.

Index Terms: cycle spinning, contourlet transform, wavelet transform, quincunx filter, directional filter banks, aliasing contourlet transform, image denoising.

الخلاصة

ان تحويل المخطط هو أحد انواع التحويل الهندسي والتي توفر لنا ميزة مهمة في معالجة الاتجاهية في الصور. لكن المرشحات المستخدمة غير مثالية مما يؤدي إلى مشاكل مهمة، أول هذه المشاكل هو وجود ظاهرة عدم الاستمرارية المزيفة وسببها هو مرشح لابلاس . ان التحويل الحاد المتمركز قام بحل هذه المشكلة باستبدال مرشح لابلاس بأخر متعدد النطاق. لكن هذا التحويل لم يقوم بحل مشكلة تغير الازاحة (وهي المشكلة الثانية) بسبب وجود رافع و خافض العينات في مرشحات لابلاس والمرشحات الاتجاهية. لذلك تم اقتراح هذا البحث لمعالجة المشكلة الثانية باستخدام مرشح المربع المخموس العالي الكفاءة و ايضا تم الغاء رافع و خافض العينات باستخدام المعادلة النبيلة. وقد اثبتت النتائج كفاءة النظام المقترح .

1. Introduction

A number of image-processing tasks are efficiently carried out in the domain of an invertible linear transformation. For example, image compression and denoising are efficiently done in the wavelet transform domain ^{[1], [2], [3]}. Owing to the good nonlinear approximation property of wavelets for piecewise smooth signals, they have been very effective in generating efficient representation of 1-D waveforms. In contrast, natural images contain singularities in the form of edges which need a more efficient transform than the wavelet transform (WT) ^{[4],[2]}. Hence, recently, some new transforms have been introduced to take advantage of this property like Contourlet transform ^[6] which proposed by Minh N. Do and Martin Vetterli is utilized to capture intrinsic geometrical structure and offer flexible multiscale and directional expansion. In the CT, a Laplacian pyramid (LP) ^{[4], [7]} serves as the first stage and directional filter banks (DFBs) ^{[4], [8]} as the second stage. The pyramidal filter bank structure of the contourlet transform has very little redundancy, which is important for compression.

However, non-ideal filter are used in the original contourlet result in significant amount of aliasing components showing up at location far away from the desired support ^{[9], [10]} and exhibit some fuzzy artifacts along the main image ridges. Yue Lu ^{[9], [10]} proposed a new construction of the contourlet, called sharp frequency localization contourlet transform (SFLCT) and alleviates the non-localization problem even with the same redundancy of the original contourlet. But (SFLCT) didn't solve the shift invariant problem caused by the downsamplers and upsamplers present in DFB. Hence, SFLCT is not shift-invariant, which is an important in image denoising by thresholding and easily causes pseudo-Gibbs phenomena around singularities ^{[9] [11]}. Shift invariant denoising can be realized through many methods like the cycle-spinning algorithm ^{[5] [9]}. Cycle-spinning, clearly, is not an efficient way to perform shift invariant denoising since the computational complexity of this procedure for an image of size $N*N$ is N^2 times that of the CT.

2. Contribution of this work

In this paper, quincunx filter banks proposed in ^[12] are applied to achieve shift invariance property in SFLCT. The High-performance quincunx filter banks are used in building the blocks of the DFB while for the Laplacian pyramid; the filter proposed in SFLCT is still used.

The quincunx filters yield linear-phase perfect-reconstruction systems with high coding gain, good analysis/synthesis filter frequency responses, and certain prescribed vanishing moment properties by using lifting based parameterization. Also to eliminate the artifacts due to the pseudo-Gibbs phenomenon in the DFB stage, the downsampling and resampling is moved to the end of the synthesis part and to the beginning of the analysis part, using the Noble identity ^[12].

3. Sharp Frequency Localized Contourlet Transform

Fig. 1 shows a flow graph of the contourlet transform. At the first stage, a Laplacian pyramid banks (LP) are used, and for the second one directional filter banks (DFB) are used [10]. Laplacian pyramid is used to capture the point discontinuities, and the directional filter banks (DFB), is used to link point discontinuities into linear structure. Note that, the frequency division in Fig.1 (b) is obtained by ideal filters. Fig.(2) explains the frequency division when non-ideal filters are combined with Laplacian pyramid. Gray regions in the figure represent the ideal passband, and patterned regions represent the aliasing frequency areas concentrated along two parallel lines ($\omega_2 = \pm\pi$). There are two reasons beyond the aliasing effect.

The first one is due to the periodicity of 2-D frequency spectrums of discrete signals. The other reason is intrinsic to the frequency partitioning of the DFB. Furthermore, if the directional filters are upsampled by 2 along each dimension, the aliasing components will be folded towards the lowpass regions, as patterned in Fig.2 (b), and concentrated mostly along two lines $\omega = \pm \frac{\pi}{2}$.

When the directional filters are combined with bandpass filter in Laplacian pyramid, the contourlet are not localized in frequency, with substantial amount of aliasing components outside of the desired trapezoid-shaped support [5] as the gray region shown in Fig.2 (d).

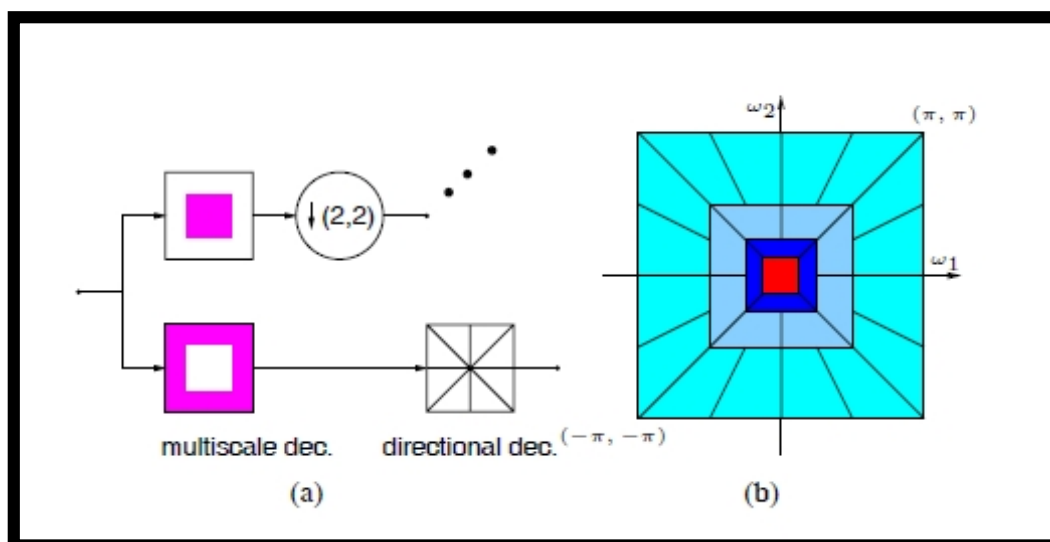


Fig.1 The Original Contourlet Transforms. (A) Block Diagram. (B) Resulting Frequency Division.

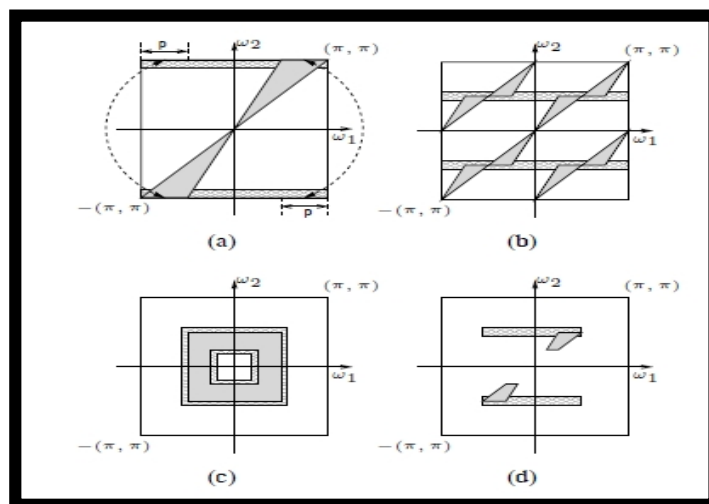


Fig.2: Spectrum Aliasing Of The Original Contourlet. (A) One Directional Filter, (B) The Directional Filter Upsampled By 2, (C)A Bandpass Filter From The Laplacian Pyramid, (D)The Resulting Contourlet Subband.

Yue Lu ^[10] proposed a new construction of the contourlet transform. An important distinction from the original contourlet is that, instead of using the Laplacian pyramid, they employed a new pyramid structure for the multiscale decomposition, which is conceptually similar to the one used in the steerable pyramid. They still use the DFB for directional decomposition as shown in Fig.(3). An important difference from the Laplacian pyramid shown in Fig.(1), the new multiscale pyramid can employ a different set of lowpass and highpass filters for the first level and all other levels. This is a crucial step in reducing the frequency-domain aliasing of the contourlet transform. The results presented in ^[10] indicate that the frequency non-localization problem is suppressed by the new construction of contourlet.

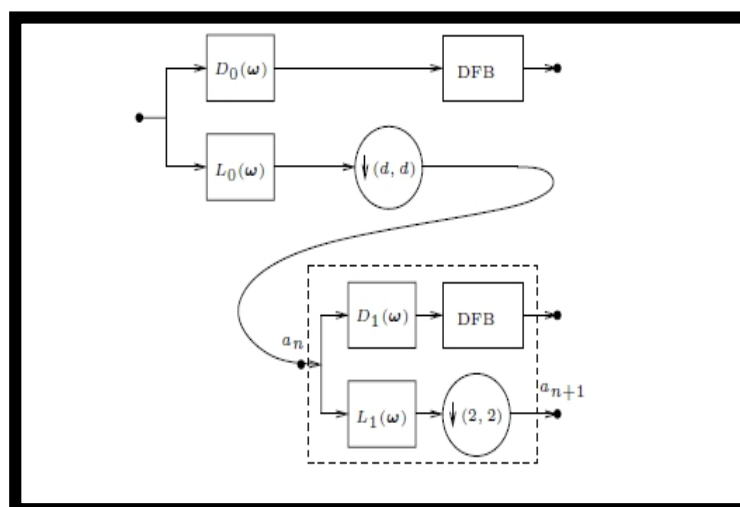


Fig. 3. The Block Diagram Of The New Contourlet Transform. Only The Analysis Part Is Shown, While The Synthesis Part Is Exactly Symmetric.

4. Developing a Shift Invariant Scheme based on Sharp Frequency Localized Contourlet Transform

It was shown in [10] that SFLCT significantly outperforms the original transform. But the drawback of SFLCT is that it still uses the DFB, hence it is not shift-invariant due to the downsamplers and upsamplers presented in the directional filter banks, which could easily produce artifacts around the singularities, e.g. edges. Thus quincunx filter banks are used in building the blocks of the DFB in SFLCT system.

4.1 Quincunx Filter Banks

Consider a shift-invariant, perfect reconstruction (PR) d-dimensional quincunx FB shown in Fig. (4)

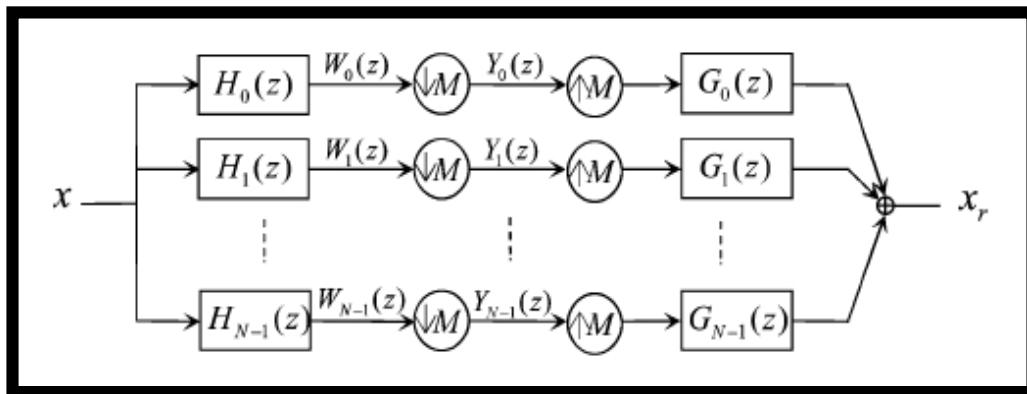


Fig. 4. Single-Level Multichannel Filter Bank.

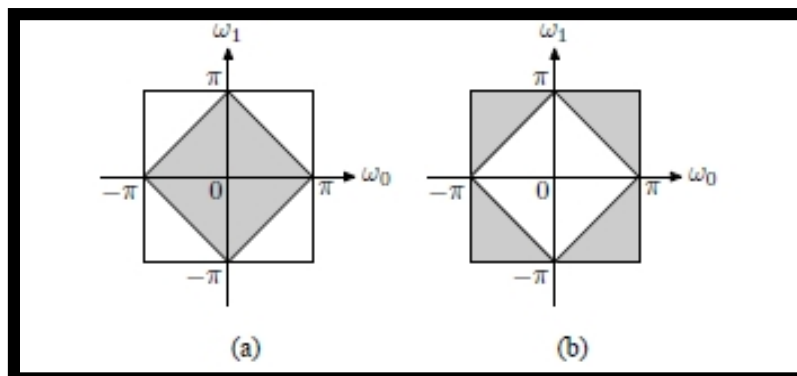


Fig.5: Ideal Frequency Responses Of Quincunx Filter Banks For The (A) Lowpass Filters And (B) Highpass Filters.

The quincunx lowpass and highpass filters are often chosen to have diamond-shaped frequency responses as shown in Figures 5(a) and (b), respectively. With the diamond-shaped frequency response, the lowpass filter can preserve high frequencies in the horizontal and vertical directions, which is a good match to the human visual system as the visual sensitivity is higher to changes in these two directions than in other directions^[8].

The shift-invariant PR condition for the quincunx UMD filter bank is

$$H_0(z)G_0(z)+H_1(z)G_1(z) = 2 \tag{1}$$

and

$$H_0(-z)G_0(z)+H_1(-z)G_1(z) = 0 \tag{2}$$

Where $\{H_k(z)\}$ and $\{G_k(z)\}$ are the analysis and synthesis filter transfer functions, respectively. M is denoted as $d \times d$ sampling matrix. If $N = d_M$, where $d_M = \det(M)$, the FB is critically sampled and if $N > d_M$, it is oversampled. The outputs of the analysis filters before downsampling is denoted as $\omega_i[n]$, for $0 \leq i < N$, where $n = (n_1, \dots, n_d)^T \in Z^d$. Hence $y_i[n] = \omega_i[M_n]$.

To prove the system is shift invariant, the following procedure is stated for obtaining all possible shifts of a multidimensional and multichannel FB. If in fig.(1), all possible shifts of $\omega_i[n]$ are computed by $k_c \in N(M)$, ($0 < c < d_M - 1$), where $d_M = \det(M)$ and $N(M)$ is the set of integer vectors of the form $Mt, t \in [0,1]^d$, then the output of the analysis section is shift invariant. It is clear that for a multilevel FB that one can apply the above method at each level for as many inputs as that level has.

According to the above procedure, if in a critically sampled FB, without loss of generality, then $\omega_i[n] = \omega_o[n + ki]$ ($0 < i < d_M - 1$) (under assumption that $k_o=0$) the FB will be shift invariant. In this case, the analysis and synthesis filters satisfy $H_i(z) = z^{k_i}H_o(z)$ and $G_i(z) = z^{-k_i}G_o(z)$ and $\{y_i[n]\}_{0 \leq i \leq d_M-1}$ represent the polyphase components of $\omega_o[n]$. Consequently, the filter bank boils down to a simple nonsubsampling system with analysis filter $H_o(z)$ and synthesis filter $G_o(z)$, where $G_o(z) = 1/H_o(z)$ to ensure perfect reconstruction. Furthermore, the redundancy of the resulting shift invariant filters bank equals N ^[4].

The DFB is realized through iterated quincunx FBs, and some resampling operations that just rearrange coefficients. In an, \hat{l} -level DFB the frequency space is decomposed to $2^{\hat{l}}$ wedge-shaped partitions (fig.6). Using the noble identities^[14], all sampling operation can be transferred to the end (beginning) of the forward (inverse) transform of the DFB. As a result, $2^{\hat{l}}$ analysis and $2^{\hat{l}}$ synthesis filters, $H_i^{(\hat{l})}$, and $G_i^{(\hat{l})}$, are obtained respectively, and the overall sampling matrices $S_i^{(\hat{l})} (1 \leq i \leq 2^{\hat{l}})$, as given below^{[15],[14]}.

$$S_i^{(i^*)} = \begin{cases} \text{diag}(2^{i^*-1}, 2), & \text{for } 1 \leq i \leq 2^{i^*-1} \\ \text{diag}(2, 2^{i^*-1}), & \text{for } 2^{i^*-1} \leq i \leq 2^{i^*} \end{cases} \quad (3)$$

In order to reduce complexity, it is appropriate to employ vertically and horizontally oriented DFBs [13][4] (fig.(6)). In *vertical DFB* (VDFB) and *horizontal DFB* (HDFB), one can achieve *mostly vertical* directions (directions between 45° and 135°) and *mostly horizontal* directions (directions between -45° and +45°), as depicted in Fig.(6). In these two modified DFB schemes, decomposing the signal horizontally or vertically is stopped after the first level of the DFB. Therefore, the overall sampling matrices for VDFB and HDFB will be

$$S_i^{V(i^*)} = \begin{cases} Q, & \text{for subband } y_1 \\ \text{diag}(2, 2^{i^*-1}), & \text{for } 2^{i^*-1} < i \leq 2^{i^*}, \end{cases} \quad (4)$$

$$S_i^{H(i^*)} = \begin{cases} \text{diag}(2^{i^*-1}, 2), & \text{for } 1 \leq i \leq 2^{i^*-1} \\ Q, & \text{for subband } y_0 \end{cases} \quad (5)$$

Where Q is the quincunx sampling matrix. The redundancy factor of the modified (either vertical or horizontal) will be $2^{i^*-1} + 1$.

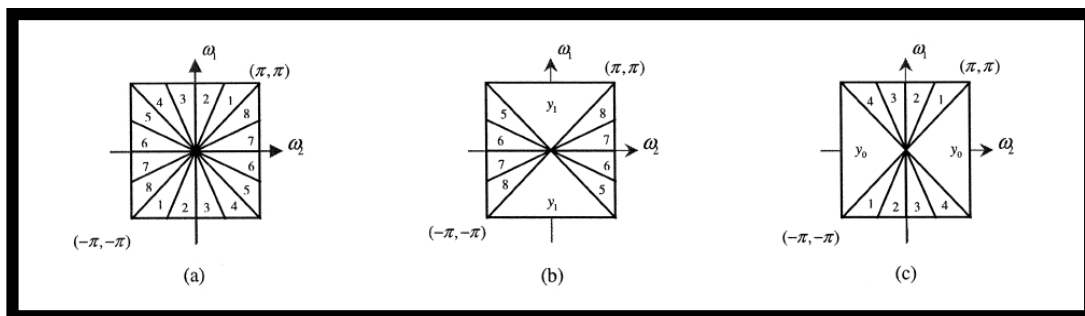


Fig.6. (A) Frequency Response Of A DFB Decomposed In Three Levels. (B) Vertical Directional Filter Banks With Three Levels. (C) Horizontal Directional Filter Banks With Three Levels.

5. Numerical Experiments

In order to demonstrate the effectiveness of the proposed design, several experiments are performed on a variety of images all of size 512X 512 and is compared with the original SFLCT [5] and contourlet (CT) [2] as well as the CS-SFLCT [9] also with the NSCT [1] is compared.

A hard threshold is performed on the subband coefficients of the various transforms. The threshold: $T_{i,j} = K \sigma_{ni,j}$ is chosen for each subband. This has been termed *K*-sigma thresholding in [1]. The images are contaminated by a zero-mean Gaussian noise with a standard deviation of σ .

From the results, one can see that although CS-SFLCT algorithm is employed to improve the denoising performance of contourlets, the computational complexity of this procedure is too high, which consequently makes this algorithm difficult for rather large-size images. In contrast, the proposed method in this paper achieves coding with less computational complexity and higher PSNR values. Also in the case of nonsubsampling CT proposed in [1], despite the system is shift invariant but the zero padding used to solve the boundary problem makes the number of samples increases due to the effect of linear convolution, resulting in an expansive transform. Although truncation can be used to obtain nonexpansive transform, it causes distortion in the reconstructed signal near the boundaries. Table (1) shows the PSNR (in dB) of the denoised images by using the above transforms. It can be seen that the method yields superior results in all cases, figure (7) shows that.

Table(1): PSNR Values Of The Denoising Experiments

Image	Noise Std. Dev.	Noisy	SFLCT	CT	CS-SFLCT	NSCT	QF-SFLCT
Lena	10	28.12	33.03	32.00	33.84	33.38	36.11
	30	18.77	27.40	26.67	28.35	28.18	33.07
	50	14.73	24.75	24.20	25.89	26.04	28.96
Barbara	10	28.11	31.38	29.90	31.36	29.18	37.45
	30	18.72	24.95	23.76	25.11	25.27	35.88
	50	14.48	22.57	21.96	23.71	23.74	30.71
Zelda	10	28.13	34.06	33.37	35.33	33.45	36.89
	30	18.83	28.67	28.24	30.67	30.00	34.19
	50	14.61	25.78	26.05	27.63	27.07	31.94

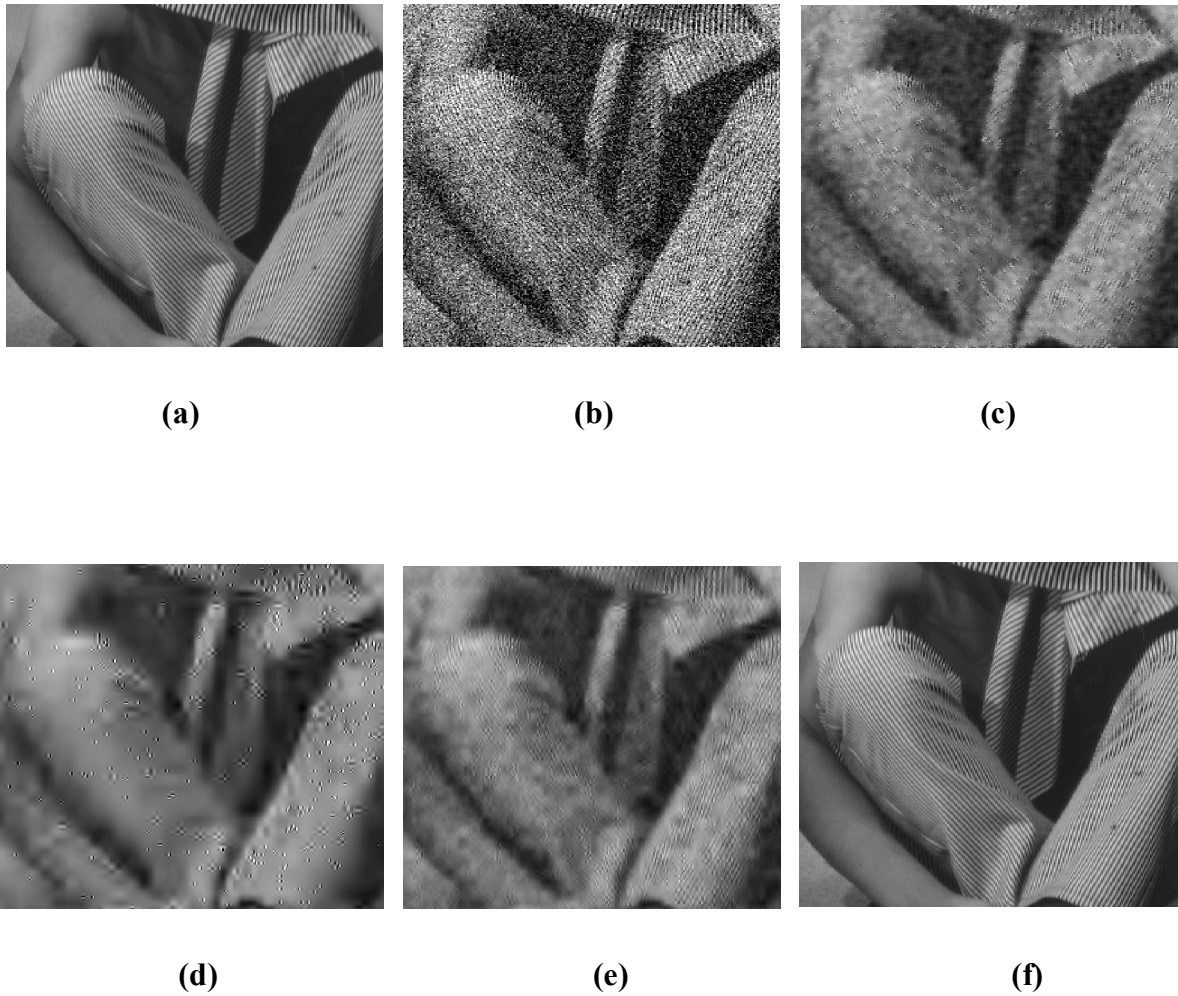


Fig. 7. Image Denoising (A) Original "Barbara" Image (B) Noisy $\Sigma=50$ (C) Denoised By CT (D) Denoised By SFLCT (E) Denoised By CS-SFLCT (F) By QF-SFLCT

6. Conclusion and Discussion

In this paper, quincunx filter bank and noble identity is employed to compensate for the lack of shift invariance property of Sharp Frequency Localized Contourlet. Experimental results show that the method is simple and outperform the other transform by eliminating the artifacts due to the pseudo-Gibbs phenomenon in the DFB stage caused by the downsampling and resampling operation.

7. References

1. Arthur L. da Cunha, Jianping Zhou, and Minh N. Do, “*The Nonsampled Contourlet Transform: Theory, Design, and Applications*” IEEE Transaction on Image Processing , Vol. 15, No. 10, PP. 3089-3101, Oct. 2006.
2. S. Mallat, “*A Wavelet Tour of Signal Processing*”, 2nd ed. New York: Academic, 1999.
3. M. Vetterli , J. Kovacicic , “*Wavelets and Subband Coding*”, Englewood Cliffs, NJ: Prentice-Hall, 1995.
4. Ramin Eslami, Hayder Radha ,” *Translation-Invariant Contourlet Transform and Its Application to Image Denoising*”, IEEE Transaction on Image Processing, Vol. 15, No. 11, PP. 3362-2006, Nov. 2006.
5. Ramin Eslami and Hayder Radha,” *The Contourlet Transform for Image De-noising Using Cycle Spinning*”, ECE Department, Michigan State University.
6. M.N. Do and M.Vetterli, “*The contourlet transform: an efficient directional multiresolution image representation*”, IEEE transaction on Image Processing, Vol.14, No. 12, PP. 2091-2106, September 2005.
7. P. J. Burt and E. H. Adelson, “*The Laplacian pyramid as a compact image code*,” IEEE Trans. Commun., vol. 31, no. 4, pp. 532–540, Apr.1983.
8. R. H. Bamberger and M. J. T. Smith, “*A filter bank for the directional decomposition of images: Theory and design*” IEEE Trans. Signal Process., vol. 40, no. 4, pp. 882–893, Apr. 1992.
9. Qu Xiaobo , Yan Jingwen ,” *The Cycle Spinning-based Sharp Frequency Localized Contourlet Transform for Image Denoising*”, 3th International Conference on Intelligent System & Knowledge Engineering-ISKE'08, July , 2008.
10. Yue Lu, M.N Do, “*A New Contourlet Transform with Sharp Frequency Localization*”, Proceedings IEEE International Conference on Image Processing, pp. 1629-1632, Atlanta, USA,2006.
11. R. R. Coifman ,D. L. Donoho, “*Translation invariant de-noising*,” *Wavelets and Statistics*, A. Antoniadis and G. Oppenheim, Eds. New York: Springer-Verlag, pp. 125–150,1995.
12. Yi Chen,” *Design and Application of Quincunx Filter Banks*”, Msc. thesis, B.Eng., Tsinghua University, China, 2002.

13. R. Eslami and H. Radha, “*New image transforms using hybrid wavelets and directional filter banks: Analysis and design*,” in *Proc. IEEE, Conf. on Image Processing*, Genova, Italy, pp. 733–736, Sep. 2005.
14. S. Park, M. J. T. Smith, and R. M. Mersereau, “*Improved structures of maximally decimated directional filter banks for spatial image analysis*” *IEEE Trans. On Image Process.*, vol. 13, no. 11, pp. 1424–1431, Nov. 2004.
15. M. N. Do and M. Vetterli, “*Contourlets*” in *Beyond Wavelets*, G. V. Welland, Ed.2 , New York: Academic, pp. 1–27, 2003.